International Journal of Polymeric Materials, 51:511–527, 2002

0091-4037/02 $12.00 + .00
DOI: 10.1080/00914030290046093

EMULSION COPOLYMERIZATION OF ACRYLONITRILE AND BUTADIENE. CALCULATION OF THE DETAILED MACROMOLECULAR STRUCTURE

V. I. Rodríguez
Facultad de Ingeniería Química, Universidad Nacional del Litoral, Argentina

D. A. Estenoz, L. M. Gugliotta, and G. R. Meira
Facultad de Ingeniería Química, Universidad Nacional del Litoral, Argentina and INTEC (Universidad Nacional del Litoral - CONICET), Argentina

A novel mathematical model is developed that predicts the detailed macromolecular structure of an acrylonitrile-butadiene rubber (NBR) produced in an industrial emulsion polymerization. The model consists of: (i) a basic module that calculates the monomer conversion and the copolymer composition; (ii) a particle size distribution module; and (iii) a macromolecular structure module that calculates the bivariate chain length distributions of the linear fraction and of each branched topology (characterized by the number of branching points per molecule). From the bivariate distributions, the univariate distributions of molecular weights, copolymer composition, and degrees of branching are obtained. The model was validated from global measurements of conversion, average molecular weights, average composition, and average degrees of branching.

Keywords: emulsion polymerization, NBR, MWD, CCD, branching distribution

1. INTRODUCTION

Important commodity polymers such as styrene-butadiene rubber (SBR) and acrylonitrile–butadiene rubber (NBR) are produced through emulsion polymerization processes. The development of mathematical models of these processes is important for their optimization and control.

Received 27 December 2000; in final form 31 December 2000.
We are grateful to PASA S. A. (Argentina) for carrying out the experimental run and for providing us with the rubber samples. We thank the financial support by CONICET, SeTCiP, and Universidad Nacional del Litoral from Argentina. Finally, our thanks to J. L. Castañeda and M. C. Brandolini (INTEC) for their help with the polymer characterization.
Address correspondence to G. R. Meira, Facultad de Ingeniería Química, Universidad Nacional del Litoral, Santiago del Estero 2829, Santa Fe (3000), Argentina.

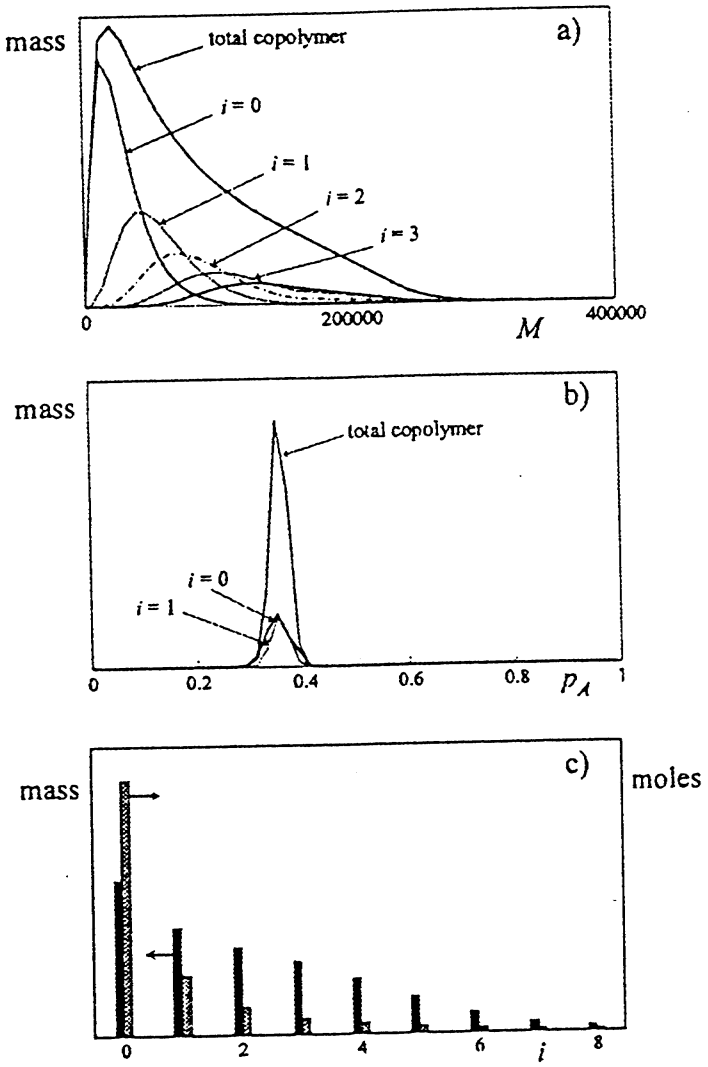

FIGURE 3 Industrial NBR Experiment. Theoretical predictions of: (a) MWDs of the total copolymer and main topologies; (b) CCDs of the total copolymer and main topologies; and (c) number- and weight-DBDs of total copolymer.

5. CONCLUSIONS

A mathematical model was developed that predicts the detailed macromolecular structure of NBR grade BJLT. The model was validated by measurements of average molecular weights, copolymer composition, and degrees of branching.

The investigated grade exhibits a negligible compositional drift and a moderate variation of the molecular weights. For each of the topologies, the average molecular weights increase and the polydispersity decreases as the number of branches increases.

The model can be applied to improve the process and/or the product quality. For example, the following could be investigated: (a) the problem of increasing the final monomer conversion without affecting the polymer quality; and (b) the controlled production of tailor-made rubbers from the point of view of their molecular architecture. Finally, the model could be

extended to simulate the synthesis of other important industrial terpolymers such as ABS or MBS.

REFERENCES

[1] Vega, J., Gugliotta, L., Bielsa, R., Brandolini, M. and Meira, G. (1997). *Ind. Eng. Chem. Res.*, **36**, 1238.

[2] Gugliotta, L., Vega, J., Antonione, C. and Meira, G. (1997). *Polym. Reac. Eng.*, **7**, 531.

[3] Dubé, M., Penlidis, A., Mutha, R. and Cluett, W. (1996). *Ind. Eng. Chem. Res.*, **35**, 4434.

[4] Saldívar, E., Dafniotis, P. and Ray, W. (1998). *J. Macromol. Sci. – Rev. Macromol. Chem. Phys.*, **C38**, 207.

[5] van Doremaele, G., van Herk, A. and German, A. (1992). *Polym. Int.*, **27**, 95.

[6] van Doremaele, G., Geerts, F., aan de Meulen, L. and German, A. (1992). *Polymer*, **33**, 1512.

[7] Tobita, H. and Yamamoto, K. (1994). *Macromolecules*, **27**, 3389.

[8] Tobita, H. and Hamielec, A. (1995). *J. Polym. Sci. - Polym. Chem. Ed.*, **33**, 441.

[9] Charmot, D. and Guillot, G. (1992). *Polymer*, **33**, 352.

[10] Teymour, F. and Campbell, J. (1994). *Macromolecules*, **27**, 2460.

[11] Arzamendi, G., Forcada, J. and Asua, J. (1994). *Macromolecules*, **27**, 6068.

[12] Arzamendi, G. and Asua, J. (1995). *Macromolecules*, **28**, 7479.

[13] Arzamendi, G., Sayer, C., Zoco, N. and Asua, J. (1998). *Polym. Reac. Eng.*, **6**, 193.

[14] Min, K. and Ray, W. (1974). *J. Macromol. Sci. - Rev. Macromol. Chem.*, **C11**, 177.

[15] Forcada, J. and Asua, J. (1990). *J. Polym. Sci. - Polym. Chem. Ed.*, **29**, 1231.

[16] Saldívar, E. and Ray, W. (1997). *Ind. Eng. Chem. Res.*, **36**, 1322.

[17] Lichti, G., Gilbert, R. and Napper, D. (1980). *J. Polym. Sci. - Polym. Chem. Ed.*, **18**, 1297.

[18] Storti, G., Polotti, G., Cociani, M. and Morbidelli, M. (1992). *J. Polym. Sci. - Polym. Chem. Ed.*, **30**, 731.

[19] Tobita, H., Takada, Y. and Nomura, M. (1994). *Macromolecules*, **27**, 3804.

[20] Salazar, A., Gugliotta, L., Vega, J. and Meira, G. (1998). *Ind. Eng. Chem. Res.*, **37**, 3582.

[21] Echevarría, A., Leiza, J., de la Cal, J. and Asua, J. (1998). *AICHE J*, **44**, 1667.

[22] Ullmann's Encyclopedia of Industrial Chemistry, Vol. A23, VCH Publishers, Inc., 1993.

[23] Ambler, M. (1976). *J. Appl. Polym. Sci.*, **20**, 2259.

[24] Estenoz, D., Valdez, E., Oliva, H. and Meira, G. (1996). *J. Appl. Polym. Sci.*, **59**, 861.

[25] Estenoz, D. A., Vega, J. R., Oliva, H. M. and Meira, G. R., Analysis of a Styrene-Butadiene Graft Copolymer by Size Exclusion Chromatography. I. Computer Simulation Study for Estimating the Biases Induced by Branching Under Ideal Fractionation and Detection, *Int. J of Pol. Charact.* (in the press).

[26] Kolthoff, I., Sandell, E., Meehan, E. and Bruckenstein, S. (1969). *Quantitative Chemical Analysis*, 4th edn., Macmillan, New York.
[27] Vega, J., Gugliotta, L., Castañeda, J. and Meira, G. (1998). *Proceedings of the IV Latin American Symposium of Polymer Science*, Viña del Mar, Chile, p. 133.
[28] Vega, J. R., Estenoz, D. A., Oliva, H. M. and Meira, G. R., Analysis of a Styrene-Butadiene Graft Copolymer by Size Exclusion Chromatography. II. Determination of the Branching Exponent with the Help of a Polymerization Model, *Int. J of Pol. Charact.* (in the press).
[29] Zimm, B. and Stockmayer, W. (1949). *J. Chem. Phys.*, **17**, 1301.
[30] Graessley, W. and Mittelhauser, H. (1967). *J. Polym. Sci. A*-2, **5**, 431.
[31] Small, P. (1975). *Adv. Polym. Sci.*, **18**, 1.
[32] Brandrup, J. and Immergut, E. (1989). *Polymer Handbook*, 3rd edn., J. Wiley & Sons, New York.
[33] Broadhead, T. (1984). Dynamic Modeling of the Emulsion Copolymerization of Styrene/Butadiene. *M. Eng. Thesis*, McMaster University, Hamilton, Ontario, Canada, 1984.

APPENDIX. MACROMOLECULAR STRUCTURE MODULE

Consider first the global mechanism of Table 2. Call B* and A* any unreacted repeating unit of B and A in the copolymer, respectively. Also, call $[A^{\cdot}] = \sum_n \sum_m [A^{\cdot}_{(n,m)}]$ and $[B^{\cdot}] = \sum_n \sum_m [B^{\cdot}_{(n,m)}]$ (with $n+m \neq 0$), the global concentrations of A- and B-terminated non-primary radicals, respectively. The rates of transfer to the copolymer are assumed proportional to B* and A*. The rate of reaction with internal double-bonds of B units is assumed proportional to B*.

From the global kinetics, the following material balances for the free-radicals can be written:

$$\begin{aligned}\frac{\mathrm{d}\{[A^{\cdot}]V\}}{\mathrm{d}t} = \{&k_{pXA}[A][X^{\cdot}] + k_{pBA}[A]([B^{\cdot}] + [B^{\cdot}_{(0,0)}]) + k_{pAA}[A][A^{\cdot}_{(0,0)}] \\ &+ k_{fAA}[A][A^{\cdot}_{(0,0)}] + k_{fBA}[A]([B^{\cdot}] + [B^{\cdot}_{(0,0)}]) \\ &- (k_{fAB}[B] + k_{fAX}[X] \\ &+ k_{fpAB}[B^*] + k^*_{pA}[B^*] + k_{pAB}[B] + k_{fpAA}[A^*])[A^{\cdot}]\}V \end{aligned} \tag{A.1}$$

$$\begin{aligned}\frac{\mathrm{d}\{[B^{\cdot}]V\}}{\mathrm{d}t} = \{&k_{pBB}[B][B^{\cdot}_{(0,0)}] + k_{pAB}[B]([A^{\cdot}] + [A^{\cdot}_{(0,0)}]) + k_{pXB}[B][X^{\cdot}] \\ &+ k_{fBB}[B][B^{\cdot}_{(0,0)}] + k_{fAB}[B]([A^{\cdot}] + [A^{\cdot}_{(0,0)}]) \\ &- (k_{fBA}[A] + k^*_{pB}[B^*] + k_{fBX}[X] \\ &+ k_{fpBB}[B^*] + k_{pBA}[A] + k_{fpBA}[A^*])[B^{\cdot}]\}V \end{aligned} \tag{A.2}$$

$$\frac{d\{[A^{\cdot}_{(0,0)}]V\}}{dt} = \{k_{fpAA}[A^*][A^{\cdot}] + k_{fpBA}[A^*]([B^{\cdot}] + [B^{\cdot}_{(0,0)}]) - (k_{pAA}[A] + k_{pAB}[B] + k_{fAB}[B] + k_{fAA}[A] + k_{fAX}[X] + k_{fpAB}[B^*] + k^*_{pA}[B^*])[A^{\cdot}_{(0,0)}]\}V \tag{A.3}$$

$$\frac{d\{[B^{\cdot}_{(0,0)}]V\}}{dt} = \{k_{fpBB}[B^*][B^{\cdot}] + k_{fpAB}[B^*]([A^{\cdot}] + [A^{\cdot}_{(0,0)}]) + k^*_{pA}[B^*]([A^{\cdot}] + [A^{\cdot}_{(0,0)}]) + k^*_{pB}[B^*][B^{\cdot}] - (k_{pBA}[A] + k_{pBB}[B] + k_{fBA}[A] + k_{fBB}[B] + k_{fBX}[X] + k_{fpBA}[A^*])[B^{\cdot}_{(0,0)}]\}V \tag{A.4}$$

$$\frac{d([X^{\cdot}]V)}{dt} = \{k_{fAX}[X]([A^{\cdot}] + [A^{\cdot}_{(0,0)}]) + k_{fBX}[X]([B^{\cdot}] + [B^{\cdot}_{(0,0)}]) - (k_{pXA}[A] + k_{pXB}[B])[X^{\cdot}]\}V \tag{A.5}$$

where V is the polymer phase volume.

Call $\bar{n}$ the average number of radicals per particle, N_p the total number of polymer particles, and N_A the Avogadro's constant. The total radical concentration is represented by the term $\bar{n}N_p/(VN_A)$. This variable is calculated through the Basic Model [1], and it is equal to the following:

$$[X^{\cdot}] + [A^{\cdot}] + [A^{\cdot}_{(0,0)}] + [B^{\cdot}] + [B^{\cdot}_{(0,0)}] = \frac{\bar{n}N_p}{VN_A} \tag{A.6}$$

Equations (A.1), (A.2), and (A.4)–(A.6) together with the pseudo-steady-state assumption allow to calculate the global concentrations of each radical type. To this effect, the concentration of comonomers and CTA in the polymer particles ([A], [B], [X], respectively), must be first calculated from the Basic Model.

Consider now the detailed mechanism of Table 2. The mass balances for every possible radical species provide:

$$\frac{d\{[A^{\cdot}_{(1,0)}(0,0)]V\}}{dt} = \{k_{pXA}[X^{\cdot}] + k_{fAA}([A^{\cdot}] + [A^{\cdot}_{(0,0)}]) + k_{fBA}([B^{\cdot}] + [B^{\cdot}_{(0,0)}])\}[A]V - \{(k_{pAA} + k_{fAA})[A] + (k_{pAB} + k_{fAB})[B] + k_{fAX}[X] + (k_{fpAB} + k_{fAA} + k^*_{pA})[B^*]\}[A^{\cdot}_{(1,0)}(0,0)]V \tag{A.7}$$

$$\frac{d\{[B^{\cdot}_{(0,1)}(0,0)]V\}}{dt} = \{k_{pXB}[X^{\cdot}] + k_{fBB}([B^{\cdot}] + [B^{\cdot}_{(0,0)}]) + k_{fAB}([A^{\cdot}] + [A^{\cdot}_{(0,0)}])\}[B]V - \{k_{pBB}[B] + (k_{pBA} + k_{fBA})[A] + k_{fBX}[X] + (k_{fpBA} + k_{fBB} + k^{*}_{pB})[B^{*}]\}[B^{\cdot}_{(0,1)}(0,0)]V \quad (A.8)$$

$$\frac{d\{[A^{\cdot}_{(0,0)}(a,b)_i]V\}}{dt} = \{k_{fpAA}[A^{\cdot}] + k_{fpAB}([B^{\cdot}] + [B^{\cdot}_{(0,0)}])\}[A^{*}(a,b)_{i-1}]V - \{(k_{pAA} + k_{fAA})[A] + (k_{pAB} + k_{fAB})[B] + k_{fAX}[X] + (k_{fpAB} + k^{*}_{pA})[B^{*}]\}[A^{\cdot}_{(0,0)}(a,b)_i]V; \quad (a,b,i = 1,2,\ldots) \quad (A.9)$$

$$\frac{d\{[B^{\cdot}_{(0,0)}(a,b)_i]V\}}{dt} = \{k_{fpBB}[B^{\cdot}] + (k_{fpBA} + k^{*}_{pA})([A^{\cdot}] + [A^{\cdot}_{(0,0)}])\}[B^{*}(a,b)_{i-1}]V - \{(k_{pBB} + k_{fBB})[B] + (k_{pBA} + k_{fBA})[A] + k_{fBX}[X] + k_{fpBA}[A^{*}]\}[B^{\cdot}_{(0,0)}(a,b)_i]V; \quad (a,b,i = 1,2,\ldots) \quad (A.10)$$

$$\frac{d\{[A^{\cdot}_{(n,m)}(a,b)_i]V\}}{dt} = \{k_{pAA}[A^{\cdot}_{n-1,m}(a,b)_i] + k_{pBA}[B^{\cdot}_{n-1,m}(a,b)_i]\}[A]V - \{(k_{pAA} + k_{fAA})[A] + (k_{pAB} + k_{fAB})[B] + k_{fAX}[X] + (k_{fpAB} + k^{*}_{pA} + k_{fpAB})[B^{*}]\}[A^{\cdot}_{(n,m)}(a,b)_i]V \quad (a,b,i = 0,1,2,\ldots); \quad (n,m = 1,2,\ldots) \quad (A.11)$$

$$\frac{d\{[B^{\cdot}_{(n,m)}(a,b)_i]V\}}{dt} = \{k_{pBB}[B^{\cdot}_{n,m-1}(a,b)] + k_{pAB}[A^{\cdot}_{n,m-1}(a,b)_i]\}[B]V - \{(k_{pBB} + k_{fBB})[B] + (k_{pBA} + k_{fBA})[A] + k_{fBX}[X] + (k_{fpBA} + k^{*}_{pB} + k_{fpBB})[B^{*}]\}[B^{\cdot}_{(n,m)}(a,b)_i]V \quad (a,b,i = 0,1,2,\ldots); \quad (n,m = 1,2,\ldots) \quad (A.12)$$

Let us represent with $A^{*}\ (a,b)_i$ and $B^{*}\ (a,b)_i$ any unreacted unit of A and B in $P(a,b)_i$, respectively. Since the number of branches per molecule is low with respect to the total number of repetitive units, then one can write: $[A^{*}(a,b)_i] \cong a[P(a,b)_i]$; $[B^{*}(a,b)_i] \cong b[P(a,b)_i]$; $[A^{*}] \cong \sum_i \sum_b \sum_a [A^{*}(a,b)_i]$; and $[B^{*}] \cong \sum_i \sum_b \sum_a [B^{*}(a,b)_i]$.

The bivariate number chain length distribution (NCLD) is obtained from the material balance for every possible copolymer species $P(a, b)_i$, as follows:

$$\begin{aligned}\frac{d\{[P(a,b)_i]V\}}{dt} &= (k_{fAB}[B] + k_{fAA}[A] + k_{fAX}[X] + k_{fpAB}[B^*] + k_{fpAA}[A^*]) \\ &\quad \times \sum_{m=0}^{b}\sum_{n=0}^{a}[A^{\cdot}_{(n,m)}(a-n, b-m)_i]V \\ &\quad + (k_{fBB}[B] + k_{fBX}[X] + k_{fBA}[A] + k_{fpBB}[B^*] + k_{fpBA}[A^*]) \\ &\quad \times \sum_{m=0}^{b}\sum_{n=0}^{a}[B^{\cdot}_{(n,m)}(a-n, b-m)_i]V \\ &\quad - \{(k^*_{pA} + k_{fpAB})([A^{\cdot}] + [A^{\cdot}_{(0,0)}]) \\ &\qquad + (k^*_{pB} + k_{fpBB})([B^{\cdot}] + [B^{\cdot}_{(0,0)}])\}[B^*(a,b)_i]V \\ &\quad - \{k_{fpAA}([A^{\cdot}] + [A^{\cdot}_{(0,0)}]) \\ &\qquad + k_{fpBA}([B^{\cdot}] + [B^{\cdot}_{(0,0)}])\}[A^*(a,b)_i]V \\ &\qquad\qquad (a, b, i = 0, 1, 2, \ldots) \end{aligned} \tag{A.13}$$

To calculate the mass of every $P(a, b)_i$ species, each of Eq. (A.13) must be multiplied by the corresponding molecular weight ($M = a\ M_A + b\ M_B$), yielding:

$$\begin{aligned}&\frac{d\{[P(a,b)_i]V(aM_A + bM_B)\}}{dt} \\ &= \Bigg\{(k_{fAB}[B] + k_{fAA}[A] + k_{fAX}[X] + k_{fpAB}[B^*] + k_{fpAA}[A^*]) \\ &\quad \times \sum_{m=0}^{b}\sum_{n=0}^{a}[A^{\cdot}_{(n,m)}(a-n, b-m)_i] + (k_{fBB}[B] + k_{fBX}[X] + k_{fBA}[A] \\ &\quad + k_{fpBB}[B^*] + k_{fpBA}[A^*]) \sum_{m=0}^{b}\sum_{n=0}^{a}[B^{\cdot}_{(n,m)}(a-n, b-m)_i]\Bigg\} \\ &\quad \times (aM_A + bM_B)V - \{(k^*_{pA} + k_{fpAB})([A^{\cdot}] + [A^{\cdot}_{(0,0)}]) \\ &\quad + (k^*_{pB} + k_{fpBB})([B^{\cdot}] + [B^{\cdot}_{(0,0)}])\}[B^*(a,b)_i](aM_A + bM_B)V \\ &\quad + \{k_{fpAA}([A^{\cdot}] + [A^{\cdot}_{(0,0)}]) + k_{fpBA}([B^{\cdot}] + [B^{\cdot}_{(0,0)}])\} \\ &\qquad [A^*(a,b)_i](aM_A + bM_B)V \quad (a, b, i = 0, 1, 2, \ldots) \end{aligned} \tag{A.14}$$

Equation (A.14) represent the weight-chain length distribution (WCLD) of each topology i. The WCLD of the total accumulated copolymer is obtained by adding up Eq. (A.14) in all i's, producing:

$$\begin{aligned}
&\frac{\mathrm{d}\{[P(a,b)]V(a\mathrm{M_A}+b\mathrm{M_B})\}}{\mathrm{d}t} \\
&= \Bigg\{ (k_{fAB}[B]+k_{fAA}[A]+k_{fAX}[X]+k_{fpAB}[B^*]+k_{fpAA}[A^*] \\
&\quad \times \sum_i \sum_{m=0}^{b} \sum_{n=0}^{a} [A_{(n,m)}^{\cdot}(a-n,b-m)_i] \\
&\quad + (k_{fBB}[B]+k_{fBX}[X]+k_{fBA}[A]+k_{fpBB}[B^*]+k_{fpBA}[A^*]) \\
&\quad \times \sum_i \sum_{m=0}^{b} \sum_{n=0}^{a} [B_{(n,m)}^{\cdot}(a-n,b-m)_i] \Bigg\} (a\mathrm{M_A}+b\mathrm{M_B})V \\
&\quad - \{(k_{pA}^*+k_{fpAB})([A^{\cdot}]+[A_{(0,0)}^{\cdot}])+(k_{pB}^*+k_{fpBB})([B^{\cdot}]+[B_{(0,0)}^{\cdot}])\} \\
&\quad \times \sum_i [B^*(a,b)_i](aM_A+bM_B)V \\
&\quad + \{k_{fpAA}([A^{\cdot}]+[A_{(0,0)}^{\cdot}])+k_{fpBA}([B^{\cdot}]+[B_{(0,0)}^{\cdot}])\} \\
&\quad \sum_i [A^*(a,b)_i](a\mathrm{M_A}+b\mathrm{M_B})V \quad (a,b=0,1,2,\ldots)
\end{aligned} \tag{A.15}$$

The weight fraction of A in each copolymer molecule is obtained from:

$$p_A = \frac{a\mathrm{M_A}}{a\mathrm{M_A}+b\mathrm{M_B}} \tag{A.16}$$

Thus, the chain lengths (a, b) in the bivariate distributions obtained through Eqs. (A.14) and (A.15), can be changed into (M, p_A) to produce the bivariate distributions of molecular weights and chemical composition. By integration of these molecular weight/chemical composition distributions, the univariate distributions of molecular weight and chemical composition are obtained. Finally, the univariate number- and weight- DBDs are obtained by integration of Eqs. (A.13) and (A.14).

The average molecular weights of the total copolymer are calculated from its bivariate NCLD, as follows:

$$\bar{M}_n = \frac{\sum_a \sum_b \sum_i [P(a,b)_i](a\mathrm{M_A}+b\mathrm{M_B})}{\sum_a \sum_b \sum_i [P(a,b)_i]} \tag{A.17}$$

$$\bar{M}_w = \frac{\sum_a \sum_b \sum_i [P(a,b)_i](a\mathrm{M_A}+b\mathrm{M_B})^2}{\sum_a \sum_b \sum_i [P(a,b)_i](a\mathrm{M_A}+b\mathrm{M_B})} \tag{A.18}$$

The following expressions allow to calculate the average mass fraction of A in the global copolymer, and the (number- and weight-) average numbers of branches per copolymer molecule:

$$\bar{p}_A = \frac{\sum_a \sum_b \sum_i [P(a,b)_i] a M_A}{\sum_a \sum_b \sum_i [P(a,b)_i](aM_A + bM_B)} \tag{A.19}$$

$$\bar{B}_N = \frac{\sum_a \sum_b \sum_i [P(a,b)_i] i}{\sum_a \sum_b \sum_i [P(a,b)_i]} \tag{A.20}$$

$$\bar{B}_W = \frac{\sum_a \sum_b \sum_i [P(a,b)_i](aM_A + bM_B) i}{\sum_a \sum_b \sum_i [P(a,b)_i](aM_A + bM_B)} \tag{A.21}$$

In this work, the emulsion copolymerization of acrylonitrile (A) and butadiene (B) is modeled with the aim of predicting the detailed macromolecular structure of the produced rubber. The new model is an extension of that presented in Ref. [1]. In that work, a "cold" emulsion copolymerization of A and B carried out in batch or semibatch reactors was simulated. The model predictions were validated by measurements from an industrial plant [1]. The base model [1] adopts the pseudo-homopolymer and pseudo-bulk assumptions for estimating the average molecular weights and the average number of branches per molecule. A simplified version of the base model was later used in combination with plant energy measurements for producing on-line estimates of conversion, copolymer composition, and average molecular weights [2]. Dubé *et al.* [3] have also modeled the NBR process; and validated the model with some limited pilot-plant experiments.

The mathematical modelling of emulsion copolymerizations was recently reviewed by Saldívar *et al.* [4]. For linear copolymers obtained through an emulsion process, it has been possible to estimate the joint distribution of molecular weights and chemical composition [5, 6]. Also, it has been possible to predict the evolution of the gel contents generated by cross-linking of a branched copolymer [7–12]. However, none of the existing copolymerization models have so far calculated the joint distributions of molecular weights, chemical composition, and degrees of branching.

Emulsion polymerizations models may be classified according to the way they deal with the radical compartmentalization [13]. Pseudo-bulk models are the simplest. The molecular weight distribution (MWD) is calculated as in a bulk process, and the total number of radicals is obtained from the product between the total number of particles and the average number of radicals per particle. Semi-compartmentalized models assume a random distribution of radicals among the polymer particles [14–16]. The partial distinction model divides the population of free radicals into shorter radicals (that can be transferred between the phases) and longer radicals (that do not escape from the particles) [13]. Finally, the most developed models consider that the chain-length distribution of free-radicals in a particle is a function of the particle diameter and the total number of radicals in that distribution [17–19].

Pseudo-bulk models have proven adequate for estimating MWDs when most of the dead polymer is produced by transfer reaction to the chain transfer agent (CTA) or "modifier" [13, 20, 21]. Fortunately, this simplifying approach is applicable to the NBR process [1, 2]. Also, it is known that most of the final NBR molecules are linear [22], and the gel fraction is practically negligible [23].

In this work, the detailed macrostructure of NBR is modelled. To this effect, an approach similar to that employed in Estenoz *et al.* [24, 25]

for the high-impact polystyrene process is followed. It basically classifies the molecular species into different topologies (characterized by the number of branching points per molecule), and it calculates the bivariate weight chain length distribution (WCLD) for each of the generated topologies.

2. THE POLYMERIZATION SYSTEM

Consider the industrial emulsion polymerization of A and B carried out at 10°C in a 21000 dm^3 batch reactor. This same polymerization has been previously considered in Ref. [2]. In the present work, the polymer samples were reanalyzed for estimating the average degrees of branching. The recipe aims at producing NBR grade BJLT, and it is presented in Table 1. Since the ratio of comonomers is close to the azeotrope, the compositional drift is

TABLE 1 Recipe for production of rubber, and its characteristics

(*a*) *Applied recipe*

Reagent	*Total load* (*Kg*)	*Initial composition* (*pphm*[a])
Acrylonitrile	2048	31.4
Butadiene	4475	68.6
Emulsifier	228	3.49
Initiator[b]	0.176	0.0027
CTA[c]	26.7	0.409
Water	11100	170.2

(*b*) *Global measurements*

	$t = 290$ *min.*	$t = 480$ *min.* (*Final product*)
x (%)	50.5	72.1
$\bar{p}_A$[d] (%)	35.4	34.2
$\bar{M}_n$ (g/mol)	64900	65200
$\bar{M}_w$ (g/mol)	191000	220000
$\bar{M}_w/\bar{M}_n$	2.9	3.4
$\bar{B}_N$	0.471[e]	0.56[f]; 0.687[e]
$\bar{B}_W$	1.414[g]	2.061[g]

[a] Parts per hundred monomer.
[b] Diisobutyl hydroperoxide.
[c] *Tert*-dodecyl mercaptan.
[d] Global mass fraction of polymerized acrylonitrile in the copolymer.
[e] Estimated from $\bar{B}_N \cong (\bar{M}_w/2\bar{M}_n) - 1$ [30, 31].
[f] Obtained as in [27].
[g] Estimated from $\bar{B}_W \cong 3\bar{B}_N$ [30].

expected to be small. The reaction was carried out as follows. First, the main reagents were emulsified and cooled to the reaction temperature. Then, the reaction was started when the initiator was loaded.

Latex samples were withdrawn during the copolymerization, and the following was determined: conversion, copolymer composition, average molecular weights, and average number of branches per molecule (see Figs. 1a–c). For the conversion samples, the latex was collected into especially-designed 20 cm^3 stainless-steel bottles fitted with a pressure-resistant rubber septa (to avoid butadiene loss) and containing small quantities of a deactivating agent (or "short-stop"). For the polymer quality measurements, about 0.5 dm^3 of latex were collected into open glass bottles containing

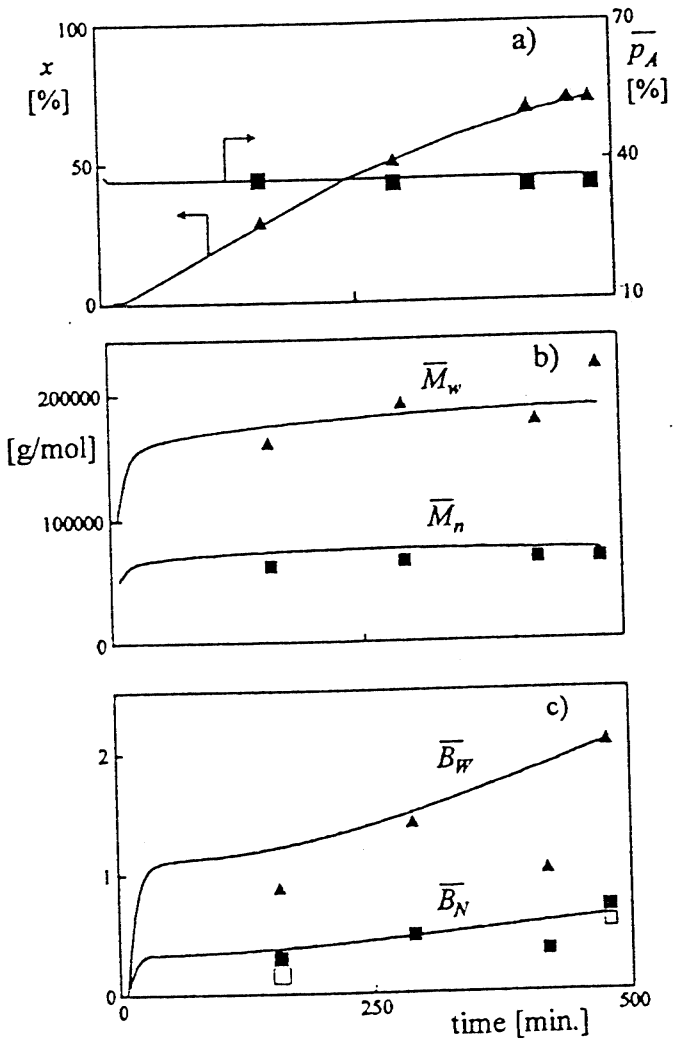

FIGURE 1 Industrial NBR Experiment. The measurements are indicated by the symbols and the model predictions are represented by the traces. (a) Evolution of the total conversion, x, and of the average mass fraction of A in the copolymer, $\bar{p}_A$. (b) Average molecular weights. (c) Number- and weight-average number of branches per molecule, $\bar{B}_N$ and $\bar{B}_W$. (The open squares indicate the $\bar{B}_N$ measurements by SEC-viscosity [27, 28]. The filled symbols indicate the indirect estimation of $\bar{B}_N$ and $\bar{B}_W$ *via* the observed polydispersity [30, 31].)

"short-stop". Water vapor was then bubbled into the latex for stripping-off the residual monomers.

At the plant laboratories, the conversion was gravimetrically determined following ASTM B 1417-80; and the global copolymer composition (or mass fraction of polymerized A) was measured through the Kjeldahl method [26]. At our laboratories, the MWD and the average degrees of branching were determined by means of a Waters ALC220 size exclusion chromatograph fitted with a Viscotek 200 on-line viscometer. The carrier solvent was tetrahydrofurane at 1 ml/min. and 25°C.

For estimating the average degrees of branching by SEC-viscometry, the following information was employed: (a) the Mark-Houwink parameters of the linear homologue; and (b) an expression interrelating the g and g' contraction factors [27, 28]. The Mark Houwink parameters were determined from intrinsic viscosity measurements of (almost linear) NBR samples taken at a low conversion. The following expression was obtained for the contraction factors: $g' = g^{0.7}$. To estimate this last exponent, the SEC measurements of g' were compared with theoretical predictions of g obtained from our global model [1] in combination with the Zimm-Stockmayer equation [27–29]. For the Zimm-Stockmayer equation, all branches were assumed trifunctional. (Previous results [1] indicate that in NBR, the global ratio of tri- to tetrafunctional branching points is close to 95:5.) Apart from the described method, the MWD measurements allowed to produce a second indirect estimation of the average degrees of branching. To this effect, analytical correlations between the average degrees of branching and the global polydispersity were used [30, 31] (see expressions at the bottom of Tab. 1). Such correlations were theoretically developed for free-radical polymerizations with negligible termination, where the main branching reaction is the chain transfer to the polymer [30, 31].

Consider the experimental results of (Figs. 1a–c). As expected, the cumulative mass fraction of polymerized A ($\bar{p}_A$), is almost constant along the reaction. Also, $\bar{M}_n$ varies moderately. This indicates that the ratio of propagation to chain transfer in the polymer particles remains relatively constant along the reaction [1]. Finally, it is seen that $\bar{M}_w$ and the number- and weight average branching points per molecule ($\bar{B}_N$ and $\bar{B}_W$, respectively) all increase along the reaction. This is to be expected, since the branching reactions increase with the monomer conversion.

3. MATHEMATICAL MODEL

The model simulates a batch (or semibatch) isothermal emulsion copolymerization of A and B. The Basic Module and the PSD Module almost coincide with those described in [1]; and for this reason they will be briefly

reviewed. All model extensions were incorporated into the new Macromolecular Structure Module.

3.1. Basic and PSD Modules

The Basic Module assumes that the aqueous phase reactions (*i.e.*, redox initiation, homopropagation of A, and radical termination) operate in parallel with the polymer phase reactions (propagation and termination). The following global variables are calculated: the volumes of the three phases (aqueous, monomer droplets and polymer particles); the concentration of the reagents in each phase; the total conversion; the mass fraction of polymer produced in the aqueous phase; the chemical composition of the instantaneous and accumulated copolymer; and the average number of radicals per particle.

The PSD Module assumes a mechanism of a simultaneous micellar and homogeneous particle nucleation, and it neglects the particle coalescence. It calculates the evolution of the total number of particles, the PSD, and the (swollen and unswollen) number-average particle diameter.

3.2. Macromolecular Structure Module

The fraction of polymer produced in the aqueous phase is less than 0.2% [1]. Thus, only the reactions in the polymer particles will be at this level considered. Also, the pseudo-bulk approach is here adopted.

The kinetic mechanism is presented in Table 2. It does not include the production nor the termination of free-radicals. Trifunctional branches are produced by transfer reactions to the polymer, while tetrafunctional branches are produced by propagation to the internal double bonds. The left column of Table 2 represents the global kinetics from the point of view of the produced copolymer. In this global scheme, P represents any copolymer molecule, while $A^{\cdot}_{(n,m)}$ and $B^{\cdot}_{(n,m)}$ respectively characterize any A- or B-ended radical with n repetitive units of A and m repetitive units of B in the new growing chain. In the detailed kinetics at the right hand side of Table 2, each copolymer molecule $P(a,b)_i$ is characterized by three integers: (i) the number of tri- plus tetrafunctional branching points per molecule, i (with $i=0$ representing the linear topology); (ii) the total number of repetitive units of A, a; and (iii) the total number of repetitive units of B, b. Also at this level, $A^{\cdot}_{(0,0)}(a,b)_i$ is a primary copolymer radical generated by transfer to an A unit of $P(a,b)_{i-1}$; $B^{\cdot}_{(0,0)}(a,b)_i$ is a primary copolymer radical generated by transfer to a B unit of $P(a,b)_{i-1}$ or by propagation to an internal double-bond of a B repeating unit; and $A^{\cdot}_{(n,m)}(a,b)_i$ or $B^{\cdot}_{(n,m)}(a,b)_i$ are respectively A- or B-ended non-primary copolymer radicals with a growing chain containing n units of A and m units of B. Finally, $A^{\cdot}_{(1,0)}(0,0)_0$

TABLE 2 The kinetic mechanism

Global kinetics $(n, m = 0, 1, 2, \ldots)$	*Detailed kinetics* $(n, m, p, q, i, j = 0, 1, 2, \ldots); (a, b = 1, 2, \ldots)$
(a) Propagation	
$X^{\cdot} + A \xrightarrow[k_{pXB}]{k_{pXA}} A^{\cdot}_{(1,0)}$	$X^{\cdot} + A \xrightarrow[k_{pXB}]{k_{pXA}} A^{\cdot}_{(1,0)}(0,0)_0$
$X^{\cdot} + B \xrightarrow{} B^{\cdot}_{(0,1)}$	$X^{\cdot} + B \xrightarrow{} B^{\cdot}_{(0,1)}(0,0)_0$
$A^{\cdot}_{(n,m)} + A \xrightarrow[k_{pAB}]{k_{pAA}} A^{\cdot}_{(n+1,m)}$	$A^{\cdot}_{(n,m)}(a,b)_i + A \xrightarrow[k_{pAB}]{k_{pAA}} A^{\cdot}_{(n+1,m)}(a,b)_i$
$A^{\cdot}_{(n,m)} + B \xrightarrow[k_{pBA}]{} B^{\cdot}_{(n,m+1)}$	$A^{\cdot}_{(n,m)}(a,b)_i + B \xrightarrow[k_{pBA}]{} B^{\cdot}_{(n,m+1)}(a,b)_i$
$B^{\cdot}_{(n,m)} + A \xrightarrow[k_{pBB}]{} A^{\cdot}_{(n+1,m)}$	$B^{\cdot}_{(n,m)}(a,b)_i + A \xrightarrow[k_{pBB}]{} A^{\cdot}_{(n+1,m)}(a,b)_i$
$B^{\cdot}_{(n,m)} + B \xrightarrow{} B^{\cdot}_{(n,m+1)}$	$B^{\cdot}_{(n,m)}(a,b)_i + B \xrightarrow{} B^{\cdot}_{(n,m+1)}(a,b)_i$
(b) Chain transfer to the monomers	
$A^{\cdot}_{(n,m)} + B \xrightarrow[k_{fAB}]{} P + B^{\cdot}_{(0,1)}$	$A^{\cdot}_{(n,m)}(a-n,b-m)_i + B \xrightarrow[k_{fAB}]{} P(a,b)_i + B^{\cdot}_{(0,1)}(0,0)_0$
$B^{\cdot}_{(n,m)} + B \xrightarrow[k_{fBB}]{} P + B^{\cdot}_{(0,1)}$	$B^{\cdot}_{(n,m)}(a-n,b-m)_i + B \xrightarrow[k_{fBB}]{} P(a,b)_i + B^{\cdot}_{(0,1)}(0,0)_0$
$A^{\cdot}_{(n,m)} + A \xrightarrow[k_{fBA}]{} P + A^{\cdot}_{(1,0)}$	$A^{\cdot}_{(n,m)}(a-n,b-m)_i + A \xrightarrow[k_{fBA}]{} P(a,b)_i + A^{\cdot}_{(0,1)}(0,0)_0$
$B^{\cdot}_{(n,m)} + A \xrightarrow{} P + A^{\cdot}_{(1,0)}$	$B^{\cdot}_{(n,m)}(a-n,b-m)_i + A \xrightarrow{} P(a,b)_i + A^{\cdot}_{(0,1)}(0,0)_0$
(c) Chain transfer to the CTA	
$A^{\cdot}_{(n,m)} + X \xrightarrow[k_{fBX}]{k_{fAX}} P + X^{\cdot}$	$A^{\cdot}_{(n,m)}(a-n,b-m)_i + X \xrightarrow[k_{fBX}]{k_{fAX}} P(a,b)_i + X^{\cdot}$
$B^{\cdot}_{(n,m)} + X \xrightarrow{} P + X^{\cdot}$	$B^{\cdot}_{(n,m)}(a-n,b-m)_i + X \xrightarrow{} P(a,b)_i + X^{\cdot}$
(d) Chain transfer to the polymer	
$A^{\cdot}_{(n,m)} + P \xrightarrow[k_{fpBB}]{k_{fpAB}} P + B^{\cdot}_{(0,0)}$	$A^{\cdot}_{(n,m)}(a-n,b-m)_i + P(p,q)_j \xrightarrow[k_{fpBB}]{k_{fpAB}} P(a,b)_i + B^{\cdot}_{(0,0)}(p,q)_{j+1}$
$B^{\cdot}_{(n,m)} + P \xrightarrow[k_{fpBA}]{k_{fpAA}} P + B^{\cdot}_{(0,0)}$	$B^{\cdot}_{(n,m)}(a-n,b-m)_i + P(p,q)_j \xrightarrow[k_{fpBA}]{k_{fpAA}} P(a,b)_i + B^{\cdot}_{(0,0)}(p,q)_{j+1}$
$A^{\cdot}_{(n,m)} + P \xrightarrow[k_{fpBA}]{k_{fpAA}} P + A^{\cdot}_{(0,0)}$	$A^{\cdot}_{(n,m)}(a-n,b-m)_i + P(p,q)_j \xrightarrow[k_{fpBA}]{k_{fpAA}} P(a,b)_i + A^{\cdot}_{(0,0)}(p,q)_{j+1}$
$B^{\cdot}_{(n,m)} + P \xrightarrow{k_{fpBA}} P + A^{\cdot}_{(0,0)}$	$B^{\cdot}_{(n,m)}(a-n,b-m)_i + P(p,q)_j \xrightarrow{k_{fpBA}} P(a,b)_i + A^{\cdot}_{(0,0)}(p,q)_{j+1}$
(e) Propagation to the polymer	
$A^{\cdot}_{(n,m)} + P \xrightarrow[k^{\cdot}_{pB}]{k^{\cdot}_{pA}} B^{\cdot}_{(0,0)}$	$A^{\cdot}_{(n,m)}(a,b)_i + P(p,q)_j \xrightarrow[k^{\cdot}_{pB}]{k^{\cdot}_{pA}} B^{\cdot}_{(0,0)}(n+a+p, m+b+q)_{i+j+1}$
$B^{\cdot}_{(n,m)} + P \xrightarrow{} B^{\cdot}_{(0,0)}$	$B^{\cdot}_{(n,m)}(a,b)_i + P(p,q)_j \xrightarrow{} B^{\cdot}_{(0,0)}(n+a+p, m+b+q)_{i+j+1}$

and $B^{\cdot}_{(0,1)}(0,0)_0$ are primary (monomer) radicals generated by transfer to A and B or by reaction between a monomer and a primary CTA radical X.

The mathematical model which is derived from the kinetics of Table 2 is presented in the Appendix. For its resolution, the results from the Basic and PSD Modules are required. The Macromolecular Structure Module calculates the (number- and weight-) bivariate chain length distributions for the total copolymer and for each of the branched topologies [Eqs. (A.13)–(A.15)]. From such bivariate distributions, the following is calculated: the global averages and the univariate distributions of molecular weights, copolymer composition (CCD), and degrees of branching (DBD). The numerical solution of Eqs. (A.13)–(A.15) involves a fixed integration step and lumping together many molecular species into

hypothetical species defined at fixed chain length intervals (*e.g.*, $\Delta a = 500$ and $\Delta b = 500$). The employed approach is similar to that previously described in [24]. The PC program was written in Watcom™ Fortran.

4. SIMULATION RESULTS

The kinetic parameters are presented in Table 3. Most of such parameters had been previously adopted in [1, 2]. The conversion x and the weight fraction of A in the copolymer $\bar{p}_A$ were obtained from the Basic Module and later verified from the distribution results [*e.g.*, through Eq. (A.19)]. According to the Basic Model, the average number of free-radicals per particle is at all times close to (but below) 0.5. As it is seen in Figure 1, the model adequately predicts the global measurements.

TABLE 3 Kinetic constants at 10°C

Parameter	*Value*	*Reference*
k_{pAA}	3.98×10^5 dm^3/mol min.	Brandrup and Immergut [32]
k_{pAB}	1.33×10^7 dm^3/mol min.	Brandrup and Immergut [32]
k_{pBA}	1.77×10^3 dm^3/mol min.	Vega *et al.* [1]
k_{pBB}	5.30×10^2 dm^3/mol min.	Vega *et al.* [1]
k_{pXA}	3.98×10^5 dm^3/mol min.	($=k_{pAA}$). Adopted in this work
k_{pXB}	1.33×10^7 dm^3/mol min.	($=k_{pAB}$). Adopted in this work
$k_{fAA} = k_{fBA}$	2.00 dm^3/mol min.	Brandrup and Immergut [32]
$k_{fAB} = k_{fBB}$	0.01 dm^3/mol min.	Broadhead [33]
$k_{fpAA} = k_{fpBA}$	1.20 dm^3/mol min.	Brandrup and Immergut [32]
$k_{fpAB} = k_{fpBB}$	0.10 dm^3/mol min.	Vega *et al.* [1]
k_{fAX}	1.28×10^5 dm^3/mol min.	Brandrup and Immergut [32]
k_{fBX}	2.41×10^2 dm^3/mol min.	Vega *et al.* [1]
$k^*_{pA} = k^*_{pB}$	9.56×10^{-3} dm^3/mol min.	Broadhead [33]

TABLE 4 Model predictions on the global characteristics of the individual topologies and the total NBR copolymer (BJLT grade)

	Weight fract. (%)	$\bar{M}_n$ (*g/mol*)	$\bar{M}_w$ (*g/mol*)	$\bar{M}_w/\bar{M}_n$	$\bar{p}_A$ (%)
$i = 0$ (linear)	28.56	30400	60600	1.99	35.4
$i = 1$	19.66	90800	133800	1.47	35.4
$i = 2$	15.91	161800	212400	1.31	35.5
$i = 3$	13.21	229400	271400	1.18	35.7
$i = 4$	10.03	278400	307500	1.10	35.7
$i = 5$	6.56	309000	328500	1.06	35.9
$i = 6$	3.65	327500	341100	1.04	36.0
$i = 7$	1.72	339100	349200	1.03	35.6
$i \geq 8$	0.70	346800	354800	1.02	35.5
Total copolymer	100.00	72100	186600	2.59	35.6

According to the model, when a copolymer molecule adds a new (tri- or tetrafunctional) branching point, then its topology is increased by one unit, and the nature of the branching point is lost. The simulation results indicate that most branches are trifunctional, with the mass fraction of copolymer with tetrafunctional branches representing only 1.45% of the total branched copolymer. Thus, each of the branched topologies (*i.e.*, with $i=1,2,\ldots$) basically represent the different trifunctional topologies.

The model predictions for the final product are presented in Table 4 and in Figures 2 and 3. At the reaction end, the linear topology is the most abundant, followed by the single-branched species. The mass fraction of molecules with more than six branches is below 2.5%. Figure 2 exhibits the bivariate WCLD of the two most abundant topologies. In Figure 3(a), the MWDs of the total copolymer and main topologies are represented. As the number of branching points increases, the average molecular weights increase, and the polydispersity decreases (Tab. 4). Figure 3(b) exhibits the CCDs of the total copolymer and two most abundant topologies. As expected, all CCDs are narrow and exhibit a common average (Tab. 4). Figure 3(c) illustrates the discrete (number- and weight-) DBDs of the total copolymer.

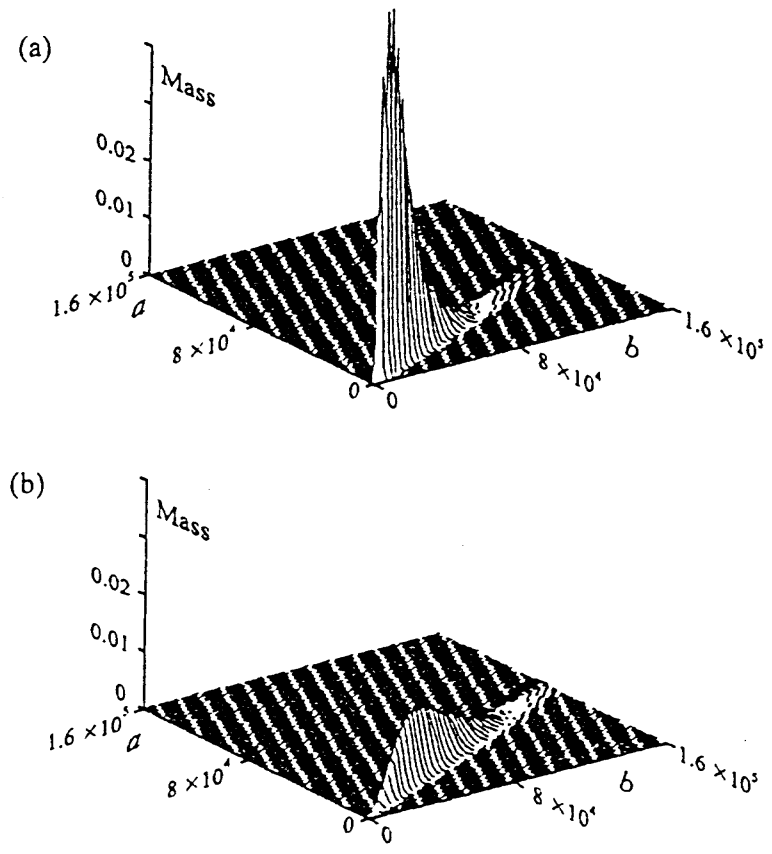

FIGURE 2 Industrial NBR Experiment. Model predictions of the bivariate WCLD at the final time for: (a) the linear topology, and (b) the single-branched topology.